ATLANTIS PRESS

Advances in Engineering Research, volume 178

Mizoram Science Congress 2018 (MSC 2018)

Focal mechanism solutions of certain earthquakes in Mizoram and its vicinity using P-wave first-motion data

Saitluanga

Department of Geology, Pachhunga University College, Aizawl 796001, Mizoram, India

Corresponding author: stasailo@gmail.com

Determination of focal mechanism solution permits characterization of the earthquake source most effectively with the estimation of fault geometry. Fault geometry is described in terms of the orientation of the fault plane and the direction of slip along the plane. However, the body wave, surface wave and the parameters such as equivalent forces at the source and seismic impulse response etc. are used to determine the orientation of fault plane and the direction of the movement associated with the earthquake. Since the majority of earthquake source processes are either complicated or cannot be observed directly, it has been necessary to find ways to determine source characteristics from seismic wave motion. The source mechanisms through P-wave first-motion data are determined by acquiring data from local seismic network supplemented by phases from the stations at teleseismic distances. Focal mechanism solutions for the events M>4.0 are well constrained. Although the uniform distribution of azimuth of a large number of stations is one of the important prerequisites for a reliable focal mechanism solution, this is not the case for the events (M<4.0) originated in NER. This situation worsens in the case of events M<3.0. Determinations of focal mechanisms for these events tend to near impossible with first motion P-wave arrival because very less number of stations record these events.

Keywords: Focal mechanism, earthquake, fault geometry, P-wave first-motion data.

INTRODUCTION

Focal mechanism solution using P-wave first-motion data is one of the simplest methods to determine fault geometry. The basic idea of this method is that, the polarity (direction) of the first P-wave arrival varies between seismic stations at different directions from an earthquake (Ligorria and Ammonm, 1999). The first motion is either compression, for the stations located such that material near the fault moves towards the station or dilatation, where the motion is away from the station. Thus, when a P-wave arrives at a seismometer from Earth's interior, a vertical component seismogram records an upward or downward first motion corresponding to either compression or dilatation (Curtis *et al.*, 2009).

The P-wave first-motion data and the azimuth of the recording stations are collected from different stations which forms the prime input to the determination of focal mechanism solution. The focal mechanism solutions of 67 numbers of events form the database for the present study. Most of these solutions are obtained from GCMT (Global Centroid Moment Tensor) database. Few solutions are determined for the present purpose by incorporating more than 45 stations data from ISC Bulletin, RRL-Jorhat and NGRI-Hyderabad seismological bulletin as well.

MATERIALS AND METHODS

Determination of focal mechanism solution using P-wave first-motion data requires maximum number of seismograms recorded by different stations. As lower magnitude event is recorded by a very few stations, higher magnitude event ($M \geq 4.0$) is generally preferred for this method. The events having magnitude $M > 4.0$ are recorded by more than 45 numbers of seismic stations including the stations at teleseismic distances. The

P and S phases are re-read from the available analogue seismograms obtained from the local seismic stations. These events are relocated based on crustal velocity model of Bhattacharya *et al*. (2005), using data for relatively larger number of seismic stations with reasonable degree of azimuthally coverage. In this study, a few focal mechanism solutions are determined (as listed in Table 1) utilizing P-wave 1st motion polarities. These are made on the basis of high precision location determination, clear record of P-wave first-motion polarity, high signal to noise ratio and recorded by maximum number of seismic stations.

Primarily, P-wave polarity, azimuth from the source, incident angle with respect to focal depth and epicentral distance in degrees etc. are the input for determination of focal mechanism solution. The P-wave first-motion data are obtained from local stations as well as stations at teleseismic distances. ISC Bulletin provides P-wave first-motion data from stations at teleseismic distances.

The fault geometry is found from distribution of first motion data on a conceptual homogeneous sphere around the focus called focal sphere. In general Wolff's net (Figure 1a) is used to project the geographical position of an observation station to a point where the tangent to the ray at the source intersects the focal sphere. The P-wave ray path leaving the source can be identified by two parameters: the azimuth from the source (f_s) and the ray parameter or take off angle, i_h (Lay *et al*., 1995). The azimuth of the direction of the ray from the source and the takeoff angle prescribes a unique path through the earth to a point on the surface and the corresponding portion of the outgoing wave front is designed to reach that point, conveying the initial motion in the associated region of the outgoing wave. Depending on the distribution of P-wave first motions, the zone of compression and dilatations are identified.

Focal mechanisms were determined using the steps as follows:

1. P-wave first-motion data are obtained from the seismograms of each recording station.
2. Azimuth (fs) and the epicentral distance (Δ) are calculated for known earthquake and recording stations.
3. The take-off angle, i_h is obtained from the table prepared by Hodgson (1953) and, Pho and Behe (1972).
4. Using fs and i_h the ray position is projected to each station on a lower hemisphere stereographic projection using Wulff's Net. Different symbols are used to indicate the P-wave first motion. Open circles are used to indicate dilatation and filled circles for compression.
5. The first motion data are rotated on the stereo net to find a meridian line that separates compression from dilations. This plane is drawn along with the pole to the plane, which projects at 90° from the plane.
6. The data plot is rotated to find a second meridian that separates dilatations and compressions and passes through the pole of the first plane.
7. Out of these two nodal planes the fault plane is ascertained based on the local geology inherited in the region.
8. The strike and dip of the fault planes are determined as illustrated in Figure 1b. Rake is calculated from the poles.
9. Pressure (P) and tension (T) axis is determined. The maximum compressive strain P is a pole lying on the plane containing the pole of the two fault planes. It lies in the dilatational quadrants 45° from the two nodal planes. The minimum compressive stress axis, T lies in the compressional quadrant 45° from the two planes.
10. The intermediate compressive stress axis, also called B axis or null axis, is determined along the line of intersection of the two nodal planes.

RESULTS

The focal mechanism solutions of 67 numbers of events form the database for the present study (Figure 2). Most of these solutions are obtained from GCMT (Global Centroid Moment Tensor) database. Few solutions are determined for the present purpose by incorporating more than 45 stations data from ISC Bulletin, RRL-Jorhat and NGRI-Hyderabad seismological bulletin as well.Distribution of dataset for the events depicting the percentage of faulting type is shown in Table 2. It is observed that the region is dominated by existence of higher percentage of strike-slip faulting. Table 1 indicates the events that comprises of focal mechanism solutions determined through first motion P-wave polarities and CMT (Centroid Moment Tensor) solution. Four solutions (black and white) are obtained through waveform inversion (Figure 2). Fault plane solutions for the events associated with the region are shown separately in Figure 3. A depth section of the beachball representing Figure 3a is shown in Figure 3b. Figure 3c, d, e, f indicate the associated nodal plane, P-axis orientation, T-axis orientation and both P- and T-axis orientation along the eastern part of the Surma valley. Most of the nodal planes are oriented along North-South while P-axis orientation is found to be along north of north-east.

The beachball presentation in Figure 3b for regions in the eastern part appears quite significant when a depth level of 41-60 km is considered. The events occurring within this depth range are characterized by the regime of dip-slip and thrust type of focal mechanisms. Figure 3c shows nodal planes of the focal mechanism solutions of the events associated with the study regions. Most of the solutions are characterized by thrust and strike slip fault.

It may be noted that in later figures as mentioned, the definition of the azimuth as would be seen in a map view is retained while the center of each line corresponds to the position in depth, of the solutions. An important observation is that P-axis orientations are pre-

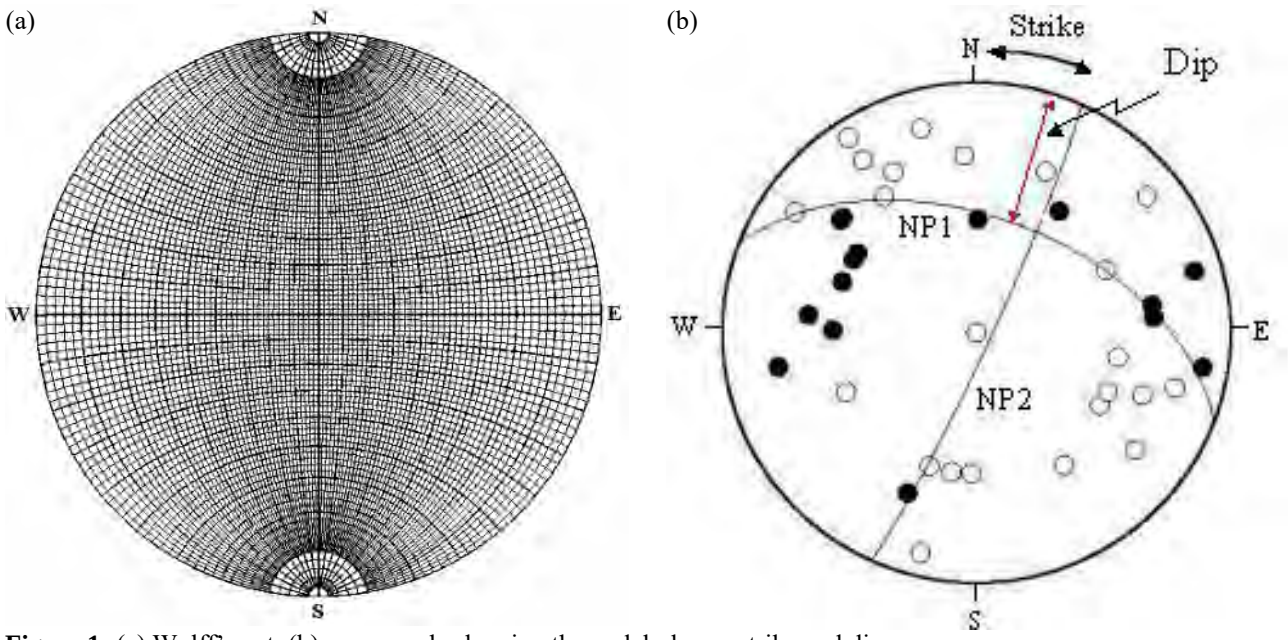

Figure 1: (a) Wulff's net; (b) an example showing the nodal planes, strike and dip.

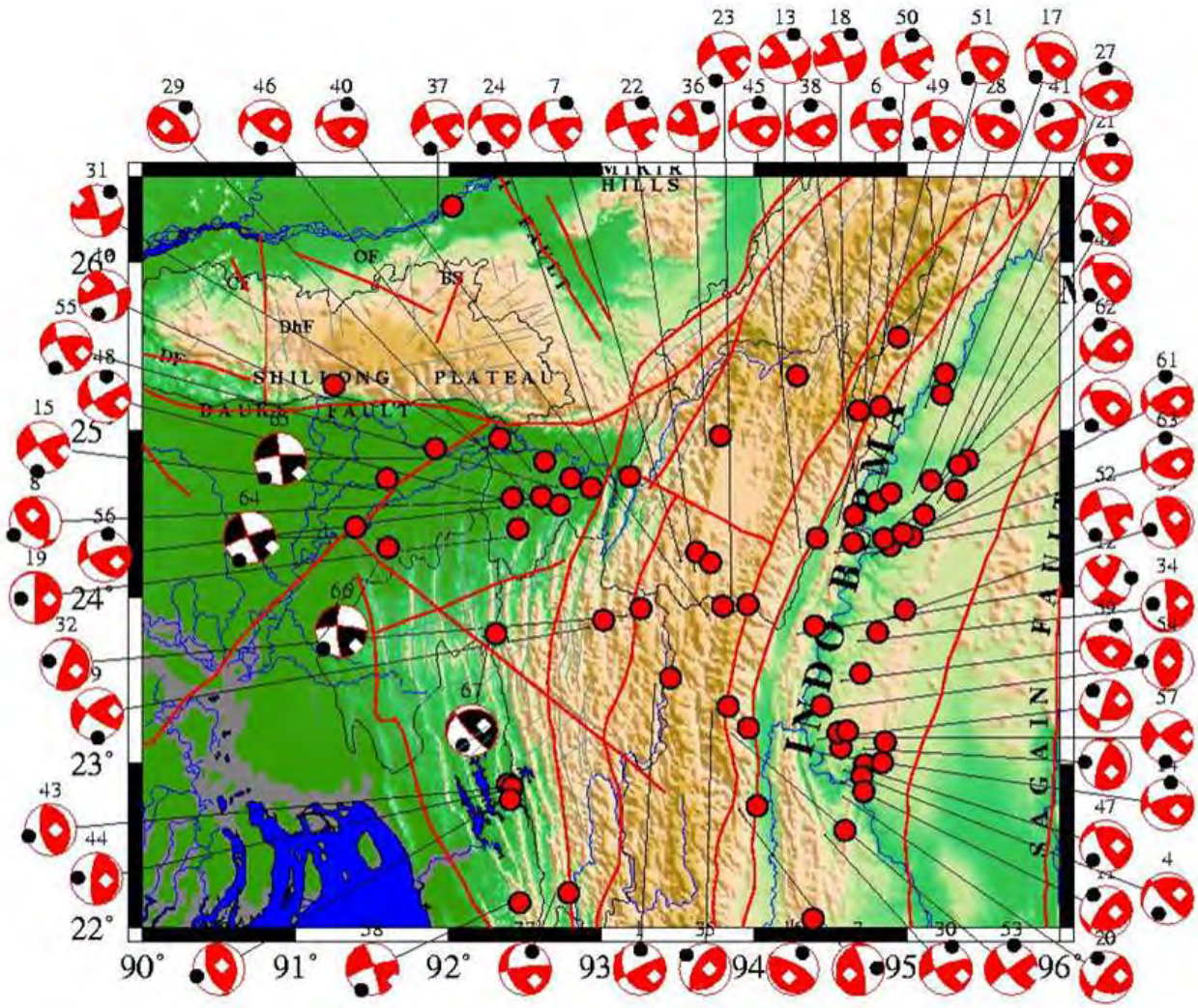

Figure 2: Beachball representation of the focal mechanism solutions in the Surma valley and its vicinity. The black colored beachball represent the focal mechanism solutions through waveform inversion whereas red coloured beachball represent the focal mechanism solution obtained from P-wave first motion.

Table 1: Parameters of the focal mechanism solutions for earthquakes in and around Surma Valley used in this study (Source: CMT and FMS determined in this study).

Year	Month	Day	Hr	Min	Sec	Lat	Long	Depth	Mag	Strike	DIP	SLIP
1977	10	13	11	32	9.3	23.48	93.35	61	5.2	145	41	171
1978	2	23	23	18	33.2	23.09	94.72	105	5.1	331	31	44
1980	11	20	18	14	11.7	22.72	93.9	33	5.3	208	19	131
1981	5	1	4	8	10.4	22.96	94.59	101	5	247	22	21
1983	8	23	12	12	16.9	24.57	95.2	126	5.1	297	44	58
1983	8	30	10	39	27.3	25.07	94.72	63	5.6	161	65	159
1984	5	6	15	19	11.4	24.22	93.52	33	5.7	157	69	161
1984	12	30	23	33	39.1	24.6	92.84	33	5.6	352	46	123
1986	2	8	0	28	53.9	23.82	92.92	33	5.2	224	62	15
1986	2	19	17	34	24.6	25.2	91.17	18	5.3	340	50	180
1986	4	26	0	25	59.6	22.89	94.57	115	4.9	87	30	136
1986	7	26	20	24	48.5	23.78	94.28	33	5.1	130	72	15
1987	5	18	1	53	51	25.26	94.18	50	5.6	67	68	14
1987	8	24	9	24	40.5	23.06	94.44	92	5.1	135	42	144
1988	2	6	14	50	42.7	24.65	91.52	15	5.8	239	76	9
1988	7	3	8	19	18.9	22.05	94.25	86	5.2	133	18	104
1988	8	6	0	36	24.6	25.14	95.12	92	6.8	284	45	55
1989	4	3	19	39	35.1	25.05	94.58	93	5.1	71	81	8
1989	4	13	7	25	36.6	24.36	92.37	33	5.2	291	6	20
1989	7	15	0	9	16	22.8	94.58	108	5.4	111	44	159
1990	1	9	18	51	28.9	24.75	95.28	118	6.1	140	32	139
1991	5	11	2	15	24.1	24.16	93.61	63	5.1	159	77	171
1991	12	4	3	27	24	23.91	93.85	70	5.2	245	68	11
1991	12	20	2	6	5.7	24.67	93.09	47	5.5	258	54	30
1992	4	15	1	32	9.8	24.3	94.91	116	5.6	281	45	56
1993	4	1	16	30	11.2	23.15	94.42	107	5.3	99	44	169
1994	8	8	21	8	31.9	24.72	95.22	127	6	111	34	120
1995	5	9	9	54	20.1	25.26	95.14	92	5.2	142	33	118
1996	11	19	0	12	18.6	24.5	92.64	50	5.5	102	34	59
1997	4	14	17	53	33.1	22.57	94.46	97	4.9	150	61	165
1997	5	8	2	53	14.7	24.89	92.25	35	5.6	78	68	4
1997	7	31	15	59	37	23.89	93.16	33	5.5	330	16	40
1997	11	21	11	23	6.3	22.21	92.7	54.4	5.9	163	37	168
1998	10	16	0	5	34.3	23.74	94.68	101.2	5.2	86	12	180
1999	2	22	11	37	49.4	23.31	93.72	65	5.1	47	35	103
1999	4	5	22	32	56.5	24.91	93.68	66.4	5.3	86	62	16
1999	10	5	17	4	44.9	26.26	91.93	33	5.3	244	68	12
2000	7	2	4	27	57	24.51	94.69	82.5	5	133	37	155
2000	10	11	9	42	9.3	23.87	94.86	116.5	5.4	343	14	98
2001	3	3	22	55	59.2	23.9	93.69	55.3	5.2	140	40	141
2001	4	10	22	8	15.5	24.63	95.04	113.4	5	8	34	28
2001	8	12	1	57	59.7	24.43	94.99	121.4	5	285	40	48
2003	7	26	23	18	18	22.85	92.31	10	5.5	338	32	82
2003	7	27	12	7	29.4	22.83	92.34	10	5.2	2	16	88
2004	10	8	21	48	5.4	24.3	94.3	69.3	4.9	139	46	147
2004	12	9	8	49	0.2	24.76	92.54	34.7	5.5	243	42	32
2005	1	18	3	2	55.1	22.97	94.7	104.7	5	271	28	31
2005	2	15	11	15	11.7	24.55	92.52	35.2	5.1	145	52	174
2005	2	15	13	5	49.8	24.43	94.54	69.7	5.2	276	61	28
2005	3	25	13	34	40	25.48	94.84	67.2	5.3	151	65	176
2005	9	18	7	25	59.5	24.56	94.78	84	5.6	271	54	38
2006	3	2	17	16	60	24.27	94.53	77.9	4.9	251	70	5
2006	3	25	20	13	30.7	23.18	93.85	61	5	142	76	176
2006	5	11	17	22	54.1	23.31	94.32	48.3	5.7	15	42	102
2006	8	12	20	46	11.3	24.66	92.71	42.8	4.9	255	61	20
2006	11	10	13	21	24.3	24.54	92.33	42.5	4.9	141	46	154
2007	5	7	5	58	33	23.16	94.48	93.7	4.6	229	69	13

2006	11	10	13	21	24.3	24.54	92.33	42.5	4.9	141	46	154
2007	5	7	5	58	33	23.16	94.48	93.7	4.6	229	69	13
2007	11	7	7	10	22	22.15	92.39	28.7	5.1	251	81	-7
2007	12	7	6	56	33.6	23.5	94.57	113.3	4.8	135	42	120
2008	1	12	22	44	47.4	22.76	92.33	33.8	5	353	35	104
2009	8	11	21	43	49.8	24.25	94.77	115	5.4	119	45	139
2009	9	3	19	51	10.5	24.29	94.73	115.5	5.7	114	46	152
2009	12	29	9	1	55.7	24.32	94.85	127.3	5.6	123	41	144

Table 2: Distribution of data set (63 earthquakes) used in the study.

Subset	Proportion of total set (per cent)	Average magnitude	Average depth (km)
Total	63	5.3	70
Reverse	47.62	5.4	80
Strike-Slip	52.38	5.3	64

Table 3: Parameters of the focal mechanism solutions for earthquakes in the eastern part of Surma valley used in this study (Source : CMT and FMS determined in this study).

Year	Lat	Long	Depth	Mag	Strike	Dip	Slip
19920521	22.98	93.34	13	3.6	45	65	15
19771013	23.27	93.16	60.8	5.4	145	41	-171
19910511	23.42	93.25	73.6	5.4	159	77	171
19860208	23.79	93.09	33	5.4	224	62	-15
19890413	24.25	91.71	33	5.4	291	6	20
20010418	24.19	91.65	56	3.9	330	40	175
19681227	24.12	91.61	29	5.2	140	72	138
19880206	24.05	91.66	31	5.8	239	76	9
19710602	23.71	91.66	46	5	119	36	90
19771013	23.48	93.35	61	5.2	145	41	171
19860208	23.82	92.92	33	5.2	224	62	15
19890413	24.36	92.37	33	5.2	291	6	20
20061110	24.54	92.33	42.5	4.9	141	46	154

dominantly north north-easterly directed. The direction of the compressional axis long the respective fault indicate the prevailing stress condition of the region. As thrust and strike-slip mechanisms dominate, these two state of mechanisms reflect N-S compression rather than E-W extension.

DISCUSSION

The source mechanisms through P-wave first-motion data are determined by acquiring data from local seismic network supplemented by phases from the stations at teleseismic distances. Focal mechanism solutions for the events M>4.0 are well constrained because of availability of required number of P-wave first motions. The uniform distribution of azimuth of a large number of stations is one of the important prerequisites for a reliable focal mechanism solution. However, this is not the case for the events (M<4.0) originated in NER. In case of these events estimated focal mechanism solutions are not well constrained due to sparse distribution of recording stations. This situation worsens in the case of events M<3.0. Determinations of focal mechanisms for these events tend to near impossible with first motion P-wave arrival because very less number of stations record these events. However, basic limitation in the study of focal mechanism through P-wave first-motion method for shallow focus earthquake arises by virtue of the very limited coverage of focal sphere by the observation data. The coverage improves with the increase in depth of focus. These constraints are observed by various researchers (Khattri, 1973; Chandra, 1978). The focal mechanism solution using P-wave first-motion data use only a fraction of information contained in body waves. On the contrary the estimation of seismic moment and moment magnitudes are not possible.

REFERENCES

Bhattacharya, P.M., Pujol, J., Majumdar, R.K., Kayal, J.R. (2005). Relocation of earthquakes in the northern region using joint hypocentre determination method.

Current Science, 89, 1404-1413.

Chandra, U. (1978). Seismicity, earthquake mechanisms and tectonics along the Himalayan mountain range and vicinity. *Physics of the Earth and Planetary Interiors*,16, 109-131.

Curtis, A., Nicolson, H., Halliday, D., Trampert, J., Baptie, B. (2009). Virtual seismometers in the subsurface of the Earth from seismic interferometry. *Nature Geoscience*, 2(10), 700.

Hodgson, J.H., Storey, R.S. (1953). Tables extending Byerly's fault plane technique to earthquakes of any focal depth. *Bulletin of the Seismological Society of America*, 43, 49-61.

Khattri, K. (1973). Earthquake focal mechanism studies – A review. *Earth Science Review*, 9, 19-63.

Lay, T., Wallace, T.C. (1995). *Modern Global Seismology*. Academic Press, New York, USA, p. 521.

Ligorria, J. P., Ammon, C. J. (1999). Iterative deconvolution and receiver-function estimation. *Bulletin of the seismological Society of America*, 89(5), 1395-1400.

Pho, T.P., Behe, L. (1972). Extended distances and angle of incidence of P-waves. *Bulletin of the Seismological Society of America*, 62, 885-902.